



Liao, W., Wagoum, A. U. K., & Bode, N. W. F. (2017). Route choice in pedestrians: determinants for initial choices and revising decisions. *Journal of the Royal Society Interface*, 14(127), [20160684].
<https://doi.org/10.1098/rsif.2016.0684>

Peer reviewed version

Link to published version (if available):
[10.1098/rsif.2016.0684](https://doi.org/10.1098/rsif.2016.0684)

[Link to publication record in Explore Bristol Research](#)
PDF-document

University of Bristol - Explore Bristol Research

General rights

This document is made available in accordance with publisher policies. Please cite only the published version using the reference above. Full terms of use are available:
<http://www.bristol.ac.uk/red/research-policy/pure/user-guides/ebr-terms/>

Supplementary information for “Route choice in pedestrians: determinants for initial choices and revising decisions”

Weichen Liao*, Armel U. Kemloh Wagoum, Nikolai W. F. Bode

Abstract

Here we present supplementary information for the article “Route choice in pedestrians: determinants for initial choices and revising decisions” published in *Journal of the Royal Society Interface*.

1. Additional Figures

Further analysis carried out on the experimental and simulated data are presented in the following figures.

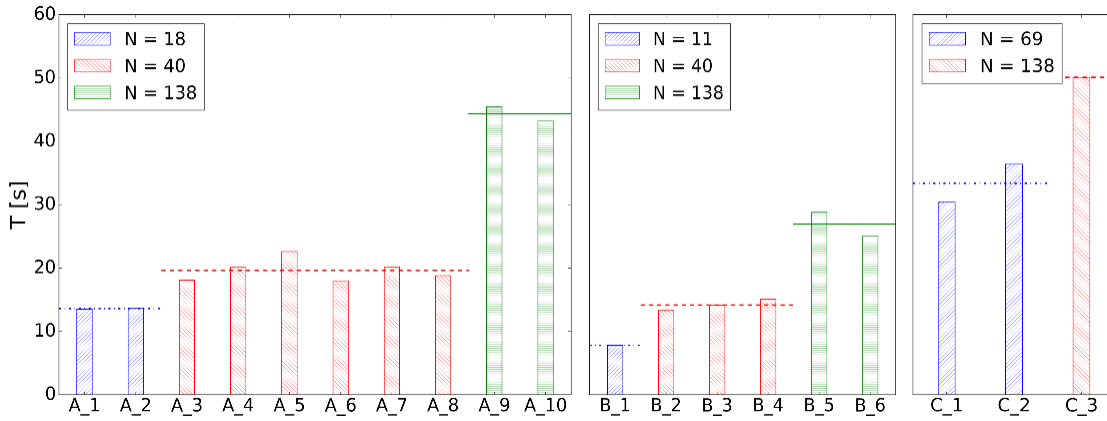


Figure S1: Summary of evacuation time T for each run in the experiments. N is the sum of N_I and N_{II} , the numbers of participants in holding areas I and II, respectively. The horizontal line denotes the average value for the runs with the same initial conditions. T is comparable within the runs with the same initial conditions. The corresponding mean \bar{T} and standard deviation $\sigma_{\bar{T}}$ are given in supplementary table S2.

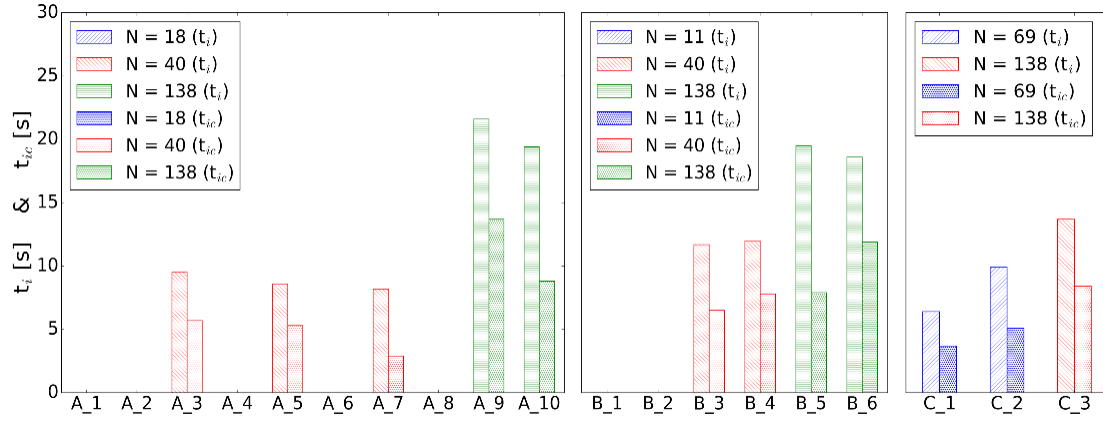


Figure S2: Mean values of t_i and t_{ic} across the n pedestrians with path re-planning behaviour in each run. t_i is the egress time for pedestrian i . t_{ic} is the time until pedestrian i changed her route. The values are calculated based on supplementary table S3. In runs for which no data is shown, no pedestrians showed path re-planning behaviour.

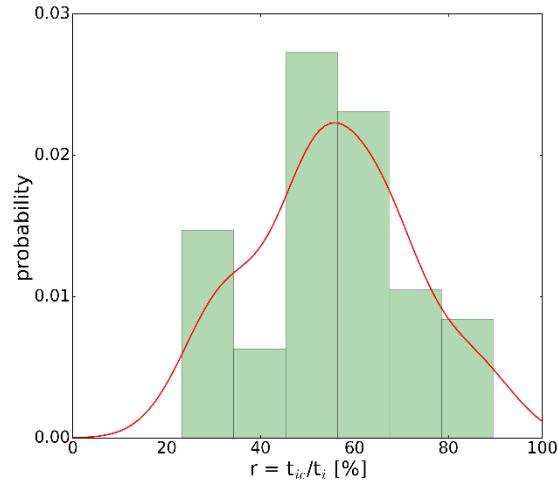


Figure S3: Observed distribution of the ratio r (r is the ratio of t_{ic} to t_i : $r = t_{ic}/t_i$ or time of change in decision over total evacuation time). The red curve represents the corresponding Gaussian kernel estimation of the histogram. According to a Kolmogorov-Smirnov test, the distribution probability is highly consistent with a normal distribution with the mean and standard deviation of 55.56% and 16.51%, respectively (see main text).

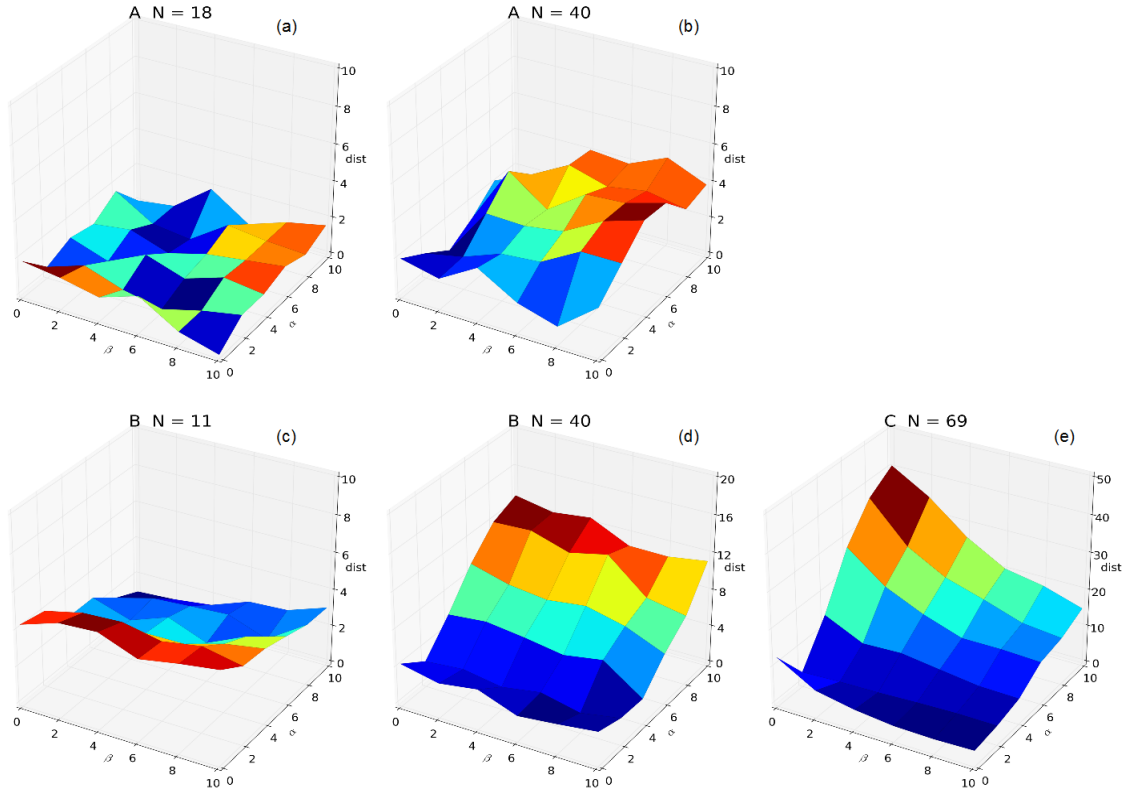


Figure S4: Part of our sensitivity analysis based on the quantity *dist* (see equation 3 in the main text). The calibration of parameters was performed on the combined data from all experimental runs in experiments A, B and C. In this figure, the simulations use $\theta = 0.5$ and $\delta = -2$ (see main text for additional information on sensitivity analysis).

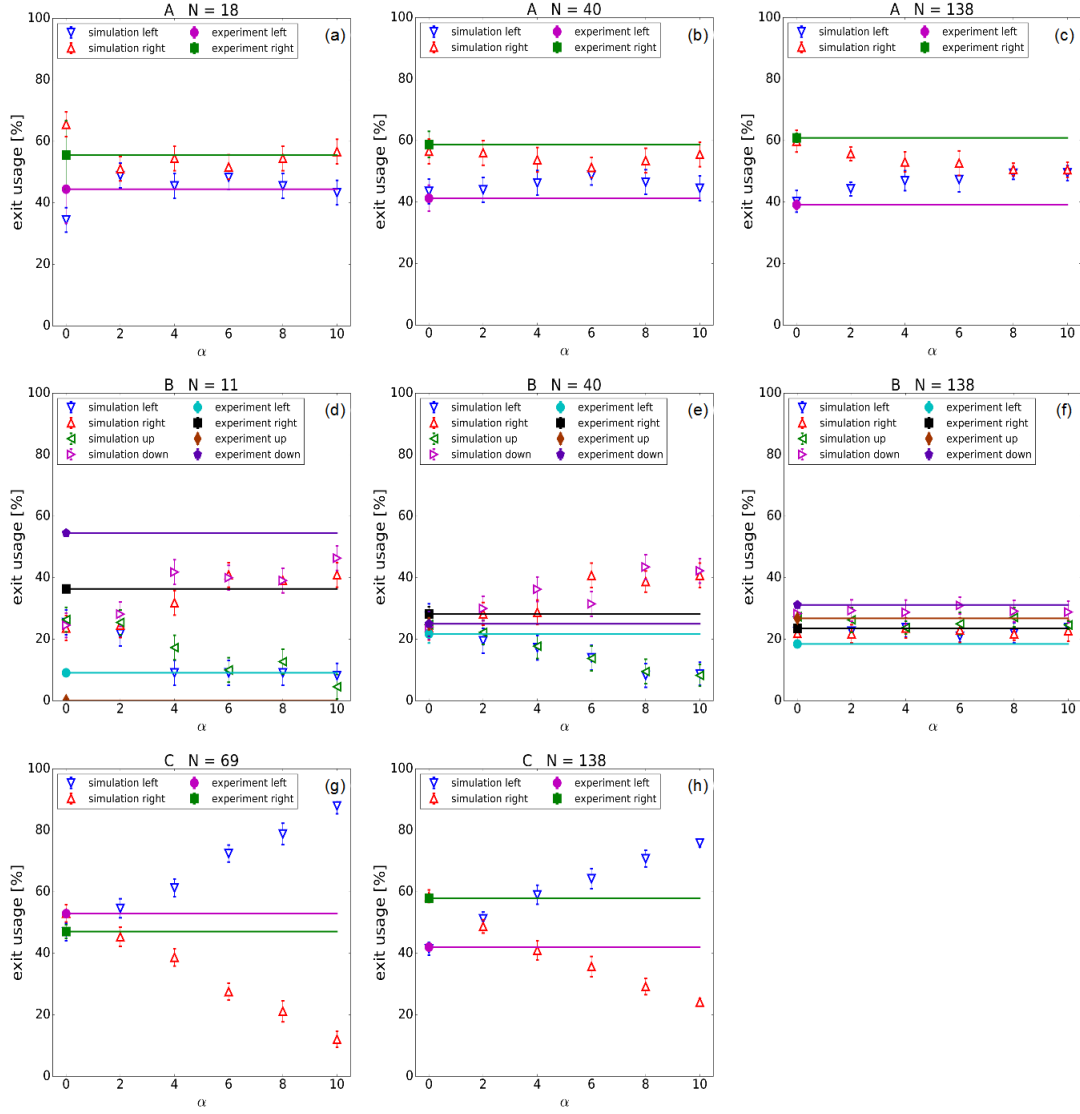


Figure S5: Sensitivity analysis for the model parameter α which controls the relative weighting of a preference for nearer exits in the initial route choice of pedestrians. Based on our parameter calibration on the combined data from experiments A, B and C, we set $\theta = 0.5$, $\delta = -2$ and $\beta = 2$. For each scenario, the simulation was conducted 10 times with pedestrians randomly distributed within their allocated starting positions (holding areas, see figure 1d-f in the main text). We report mean values across replicates alongside one standard deviation. The experimental data are the average value for the runs with the same initial conditions.

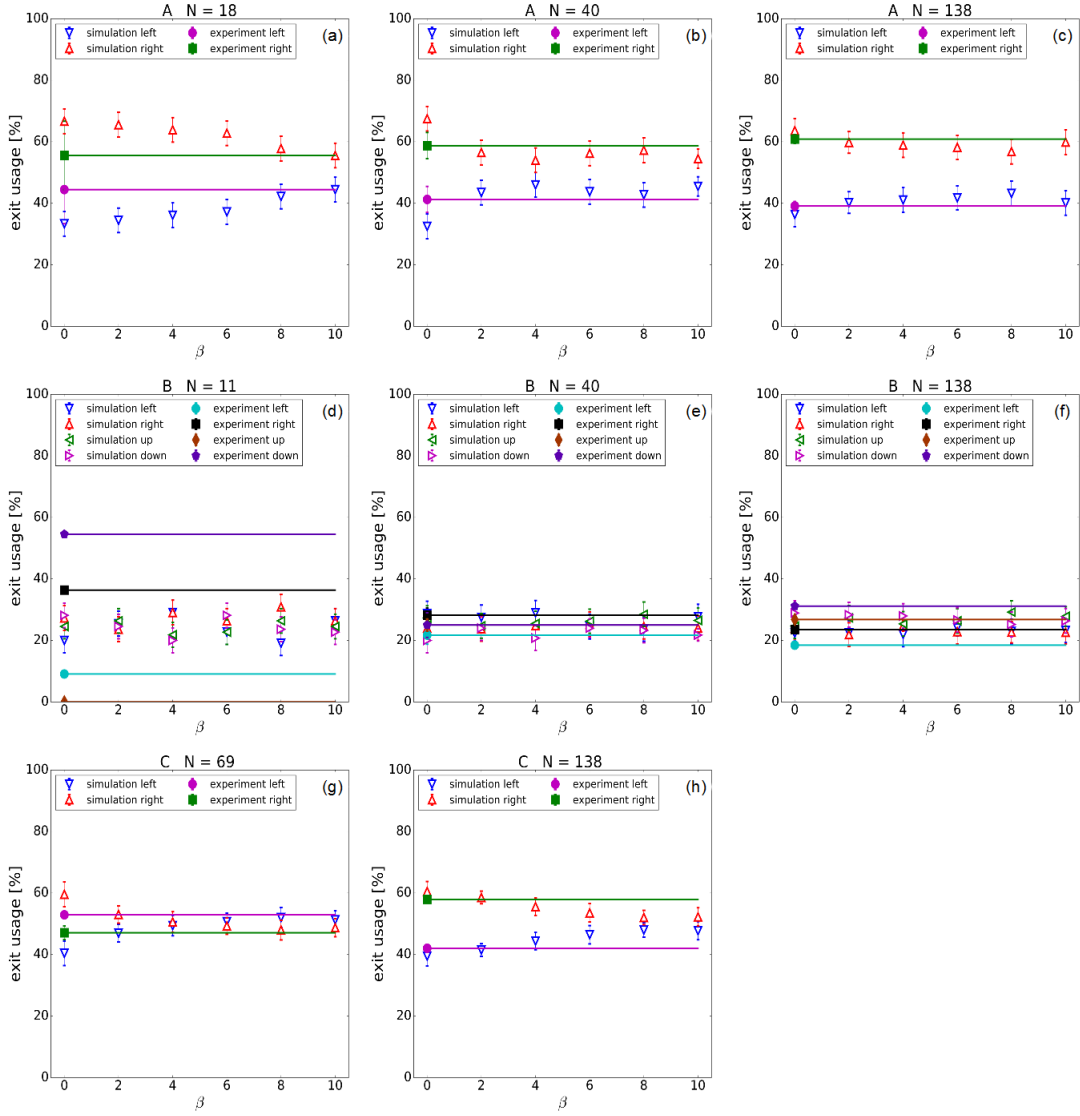


Figure S6: Sensitivity analysis for the model parameter β which controls the relative weighting of pedestrians avoiding crowded exits in their initial route choice. Based on our parameter calibration on the combined data from experiments A, B and C, we set $\theta = 0.5$, $\delta = -2$ and $\alpha = 0$. For each scenario, the simulation was conducted 10 times with pedestrians randomly distributed within their allocated starting positions (holding areas, see figure 1d-f in the main text). We report mean values across replicates alongside one standard deviation. The experimental data are the average value for the runs with the same initial conditions.

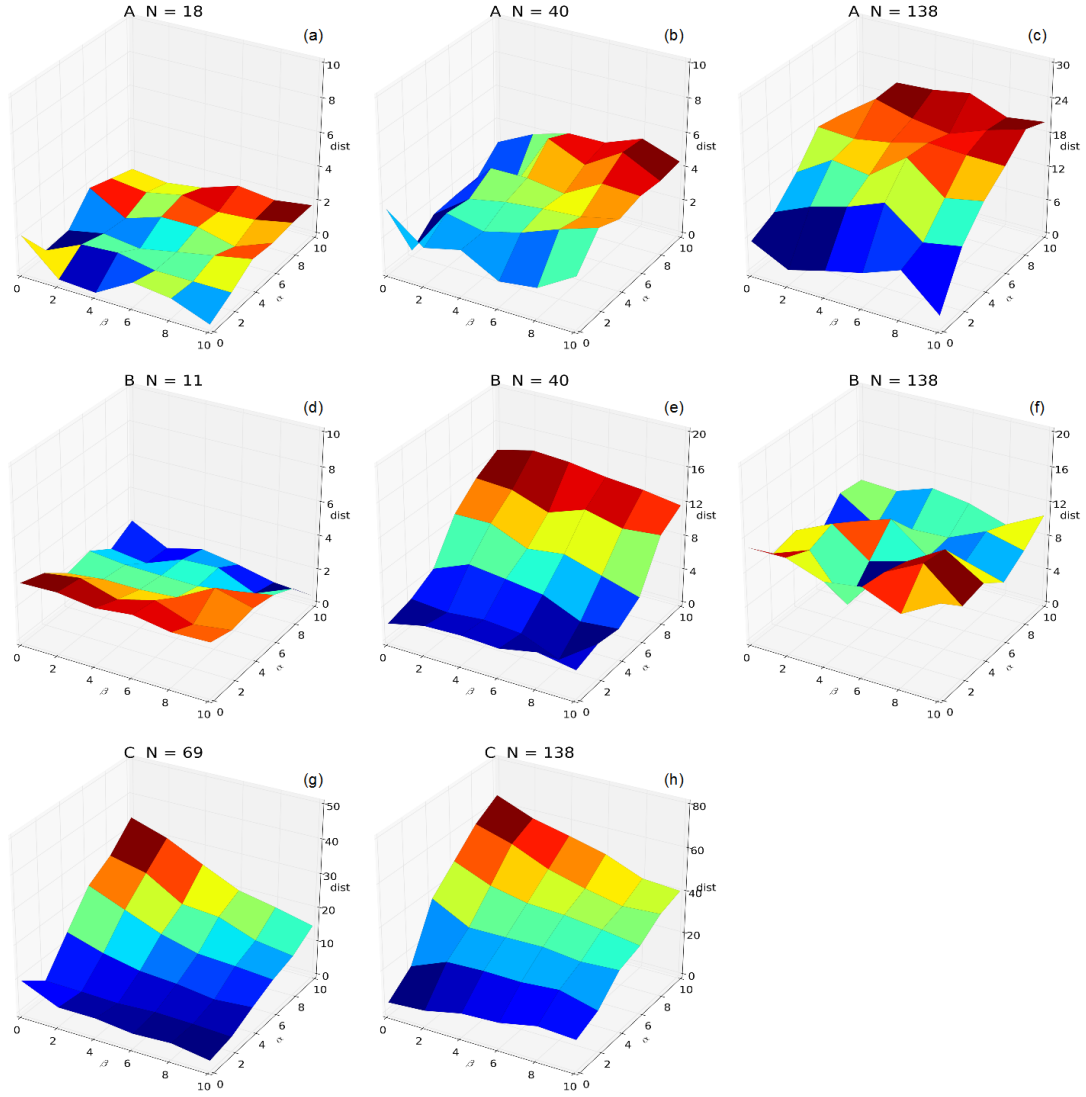


Figure S7: Sensitivity analysis based on the quantity *dist* (see equation 3 in the main text) for experiments A, B and C, respectively. The calibration of parameters was performed separately for each scenario with different numbers of pedestrians. The values of the parameters θ and δ used in the simulations shown here are listed in supplementary table S4.

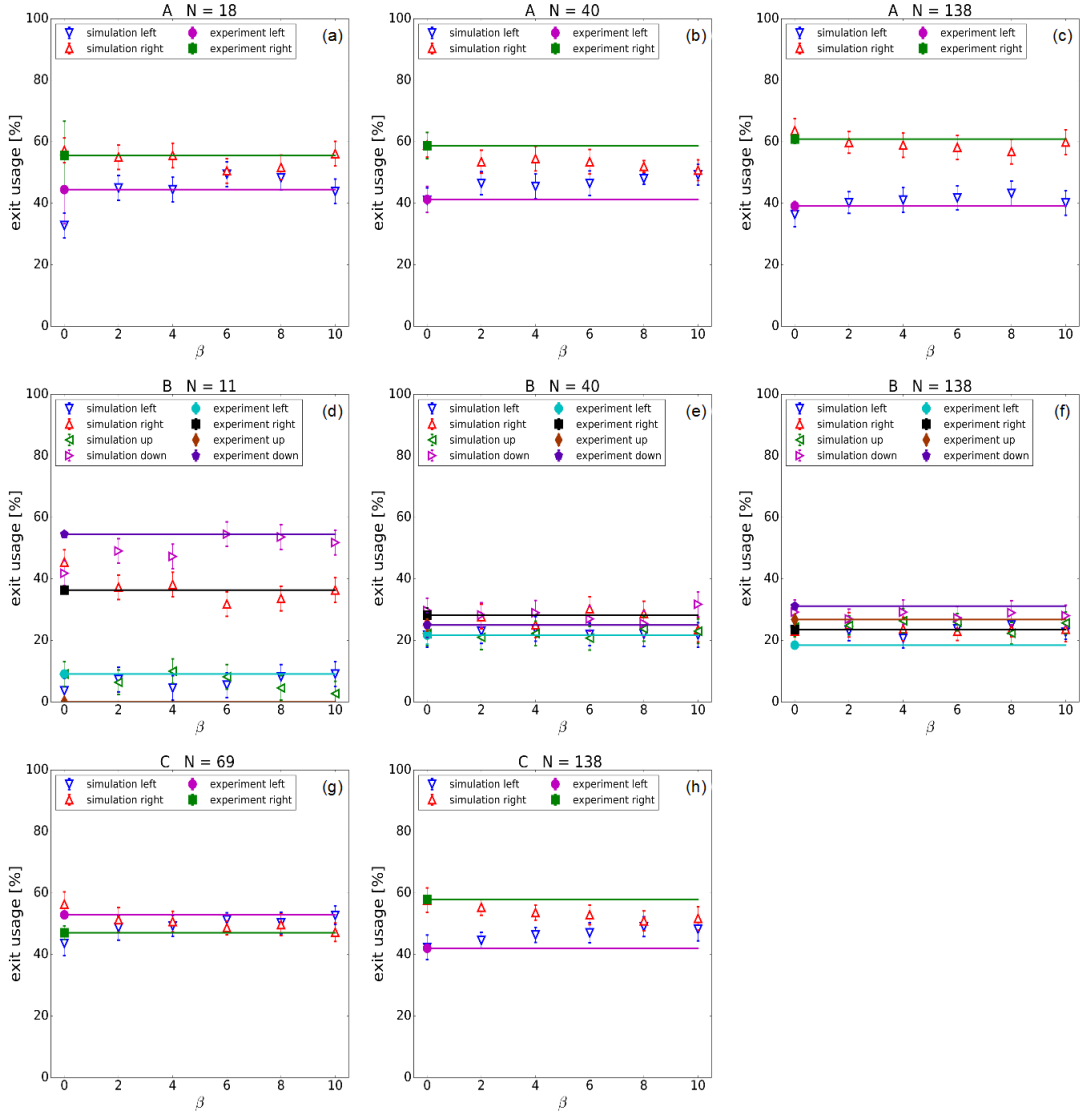


Figure S8: Sensitivity analysis for the model parameter β which controls the relative weighting of pedestrians avoiding crowded exits in their initial route choice. The parameter calibration was performed separately for each experiment A, B and C and number of pedestrians, respectively (as in figure 5 in the main text and supplementary figure S7). The parameters sets that minimised *dist* for each scenario are listed in supplementary table S4. For each scenario, the simulation was conducted 10 times with pedestrians randomly distributed within their allocated starting positions (holding areas, see figure 1d-f in the main text). We report mean values across replicates alongside one

75 standard deviation. The experimental data are the average value for the runs with the same initial
76 conditions.

77

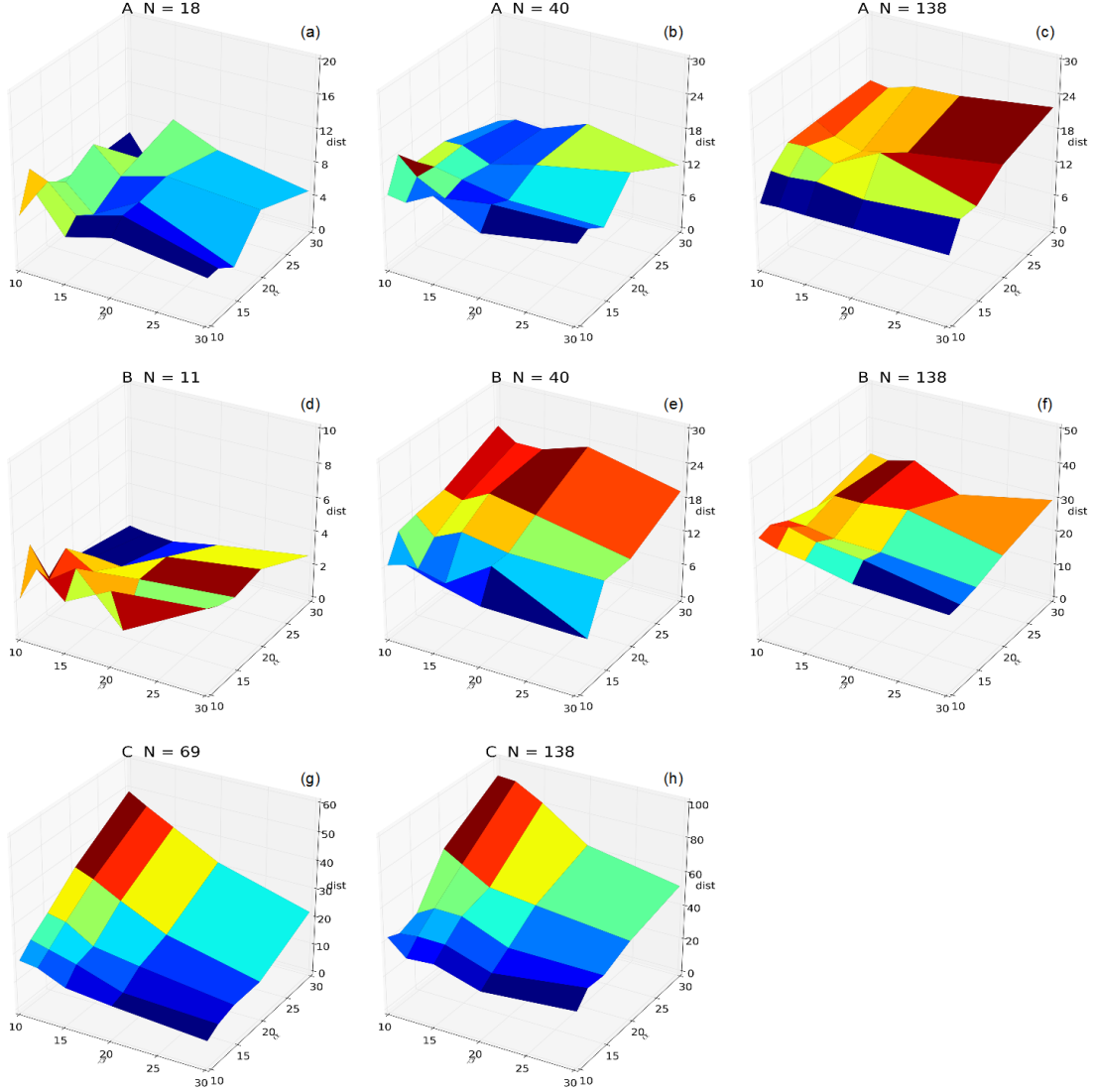


Figure S9: The calibration presented in the main text does not require simulations to capture the number of pedestrians who used the exit closest to them. Here we illustrate the effect of taking this into account by extending equation 3 in the main text:

$$dist = \sqrt{dist_{ExitUsage}^2 + dist_n^2 + dist_{Nearest}^2}, \quad (S1)$$

where $dist_{Nearest}$ is the averaged differences between experiments and simulations in the number of pedestrians who egressed through the exit closest to their initial position. We also extend the range of parameter values, as the parameter values achieving the closest match to the experimental data in our previous calibration sometimes occurred at the boundary of their ranges (e.g. $\delta = -2$, as

well as $\alpha = 10$ and $\beta = 10$). We keep the range of values for θ and enlarge those of the other three parameter values to: $\delta = (-30, -20, -15, -10, -5, -2)$, $\alpha = (10, 12, 15, 20, 30)$ and $\beta = (10, 12, 15, 20, 30)$. We then calibrate the model parameters using the combined data from all experiments and participant numbers based on the quantity *dist* shown in equation S1. The set of parameters that minimises *dist* is $\theta = 0.7$, $\delta = -10$, $\alpha = 15$ and $\beta = 30$. This is in agreement with the results from our previous calibration ($\theta = 0.5$, $\delta = -2$, $\alpha = 0$ and $\beta = 2$), insofar as suggesting a low frequency of path re-planning behaviour ($\theta = 0.5$), as well as a preference for wider exits ($\delta < 0$) and less crowded exits ($\beta > 0$). However, this new calibration also suggests that taking into account the number of pedestrians who chose their nearest exit, ensures that proximity to exits has to be included into the model ($\alpha > 0$).

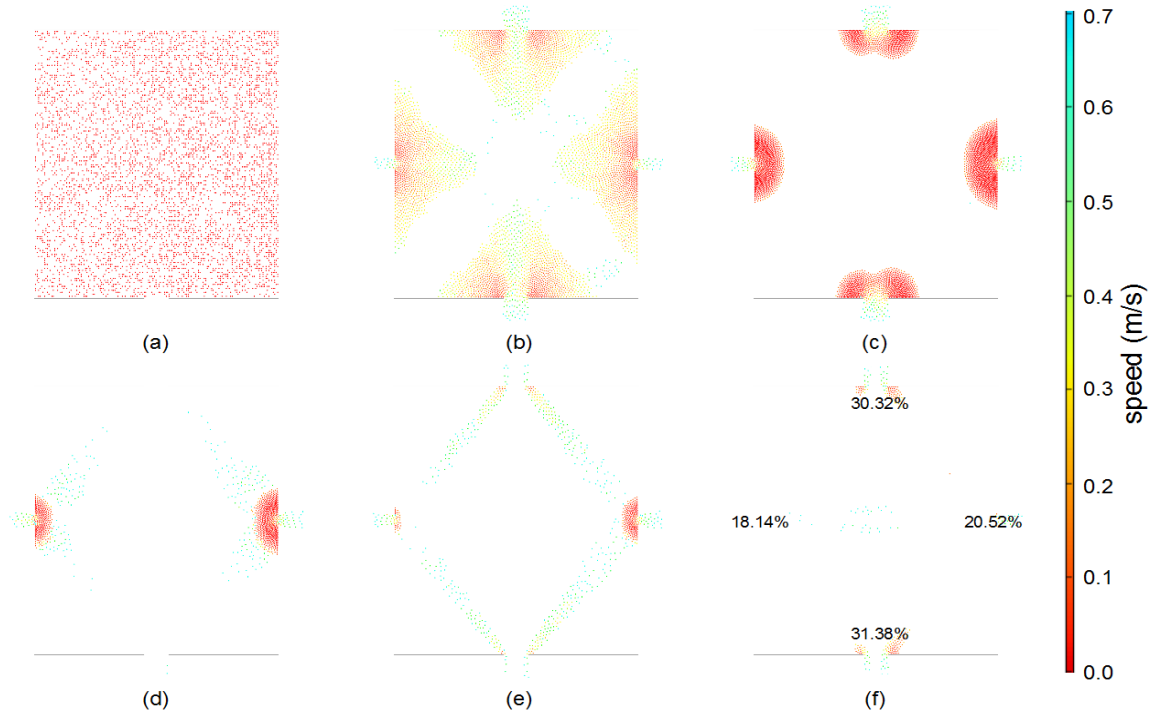


Figure S10: To demonstrate that our model is robust and can be extended to larger crowds, we performed additional simulations with $N = 5000$ agents. The scenario we considered is similar to experiment B (figure 1e in the main text), but in a room with dimensions $30 \text{ m} \times 30 \text{ m}$. The left and right hand exits are 2 m wide, and the top and bottom exits are 5 m wide. The parameter values used here are $\theta = 0.15$, $\delta = 0$, $\alpha = 8$ and $\beta = 6$. Panels show different time points in the simulation: (a) $t = 0 \text{ s}$, (b) $t = 10 \text{ s}$, (c) $t = 50 \text{ s}$, (d) $t = 130 \text{ s}$, (e) $t = 150 \text{ s}$ and (f) $t = 180 \text{ s}$. The speed of agents in meters per second is presented according to the colour scale. At the start of simulations, all pedestrians are uniformly randomly distributed in the experimental layout (a). Early in the simulation the dynamics are dominated by individuals' initial choice of route (panels b and c). Dynamic route choice processes can be observed in later stages of the simulation (d), (e) and (f). The distribution of pedestrians over exits is indicated in (f). As a result of dynamic route planning, the wider exits are used more frequently which broadly agrees with our experimental findings.

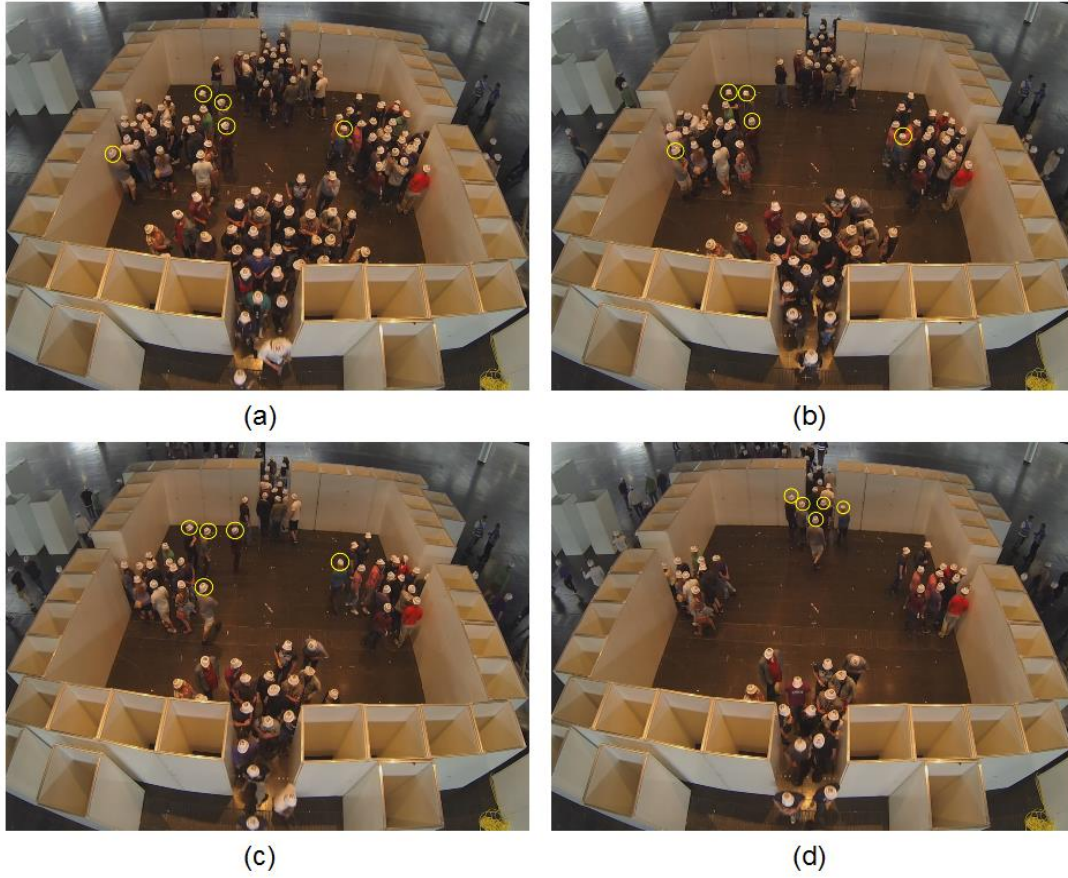


Figure S11: Illustration of path re-planning behaviour observed in experiments. Snapshots for experiment B_6 at (a) $t = 9$ s, (b) $t = 13$ s, (c) $t = 15$ s and (d) $t = 18$ s. The yellow circles mark pedestrians with path re-planning behaviour based on jam-avoidance. Jams are observed in front of exits when the total number of the participants is large enough. Pedestrians in front of exits may have to wait in or near the jams for some time. In this situation, a number of the pedestrians who arrive late into the jam may become impatient and try to search for other exits with shorter jams. (a) The yellow-marked pedestrians are waiting at their originally chosen exits. (b) After 4 s they are looking for new target exit with longer path length but smaller jam size (discernible from head-turns, difficult to see in the image). (c) Subsequently, they start to move towards a new target exit after 2 s and they reach their new target exit 3 s later (d).



Figure S12: Illustration of path re-planning behaviour observed in experiments. Snapshots for the experiment A_1 at (a) $t = 8$ s, (b) $t = 11$ s, (c) $t = 12$ s, (d) $t = 15$ s, (e) $t = 16$ s and (f) $t = 17$ s. The yellow, blue and red circles mark pedestrians with path re-planning behaviour who appear to display a range of behaviours, including time-estimating behaviour, following behaviour and route-comparing behaviour.

By ‘time-estimating behaviour’ we mean an anticipation of jam-avoidance behaviour. Pedestrians try to estimate the overall time they need to exit through the target exit before they arrive there. If this estimated time is longer than a reference time, the pedestrian might change their route. An example is given here, where the yellow-marked pedestrian appears to estimate these times when approaching the left-hand exit in the image (a,b), and then changed their decision to another exit before getting stuck in the jam in front of the original target exit (c,d).

By ‘following behaviour’ we mean that a pedestrian might change their route choice because of other pedestrians. This phenomenon could be caused by following a family member or a friend to stay together. For example, in video recordings we observed that a man in a couple persuaded the woman to follow him when changing his route. Moreover, this phenomenon could also be caused by following a stranger to minimize the evacuation time. An example is given here, where the blue-marked pedestrian appears to follow the yellow-marked pedestrian (c,d).

It appears that people show different degrees of ‘route-comparing behaviour’ during their movement. Pedestrians with a higher sense of competition may continue to compare exit routes even if they are already very close to an exit. An example for this behaviour could be given by the red-marked pedestrian who is comparing the left and right exits until he almost arrived at the original target exit (based on head turns, panels a-e). Presumably based on a last-minute comparison, this pedestrian changes their route choice when already very close to an exit (f).

2. Additional Tables

Table S1: Initial conditions for each run in the experiments. w_{left} , w_{right} , w_{up} and w_{down} are the widths of the left, right, up and down exits, respectively. N_{I} and N_{II} are the number of participants in the holding area I and II, respectively. The difference between C_1 and C_2 is only 4 participants in N_{I} . Thus these two runs are regarded to have the same initial conditions ($N_{\text{I}} = 69$ persons) in the following analysis.

Index	N_{I} [persons]	N_{II} [persons]	w_{left} [m]	w_{right} [m]	w_{up} [m]	w_{down} [m]
A_1 ~ A_2	18	0	0.7	1.1	-	-
A_3 ~ A_8	40	0	0.7	1.1	-	-
A_9 ~ A_10	48	90	0.7	1.1	-	-
B_1	11	0	0.8	0.8	0.8	0.8
B_2 ~ B_4	40	0	0.8	0.8	0.8	0.8
B_5 ~ B_6	0	138	0.8	0.8	1.2	1.2
C_1	67	0	0.8	0.8	-	-
C_2	71	0	0.8	0.8	-	-
C_3	90	48	0.8	1.2	-	-

158 Table S2: Mean \bar{T} and standard deviation $\sigma_{\bar{T}}$ of the evacuation time T for the runs with the same
159 initial conditions. N is the total number of the participants in each run.

Index	N [persons]	\bar{T} [s]	$\sigma_{\bar{T}}$ [s]
A_1 ~ A_2	18	13.6	0.1
A_3 ~ A_8	40	19.6	1.6
A_9 ~ A_10	138	44.4	1.1
B_1	11	7.8	-
B_2 ~ B_4	40	14.2	0.7
B_5 ~ B_6	138	27.0	1.8
C_1 ~ C_2	69	33.4	3.0
C_3	138	50.1	-

160

161

Table S3: Time-related information about the pedestrians with path re-planning behaviour for each run in the experiments. t_i is the evacuation time for pedestrian i . t_{ic} is the time until pedestrian i changed her route. r is the ratio of t_{ic} to t_i : $r = t_{ic}/t_i$. The mean values of t_i and t_{ic} for each run are plotted in supplementary figure S3.

Index	t_i [s]	t_{ic} [s]	r [%]	Index	t_i [s]	t_{ic} [s]	r [%]	Index	t_i [s]	t_{ic} [s]	r [%]
A_1	-	-	-	B_1	-	-	-		5.9	3.1	51.6
A_2	-	-	-	B_2	-	-	-	C_1	6.0	2.9	49.0
	8.6	3.8	44.2		11.2	5.9	52.2		7.2	5.1	69.8
A_3	9.0	4.8	53.5	B_3	11.9	5.9	49.5		9.0	4.8	52.8
	10.8	8.4	77.9		11.9	7.8	64.9	C_2	10.4	5.7	54.5
A_4	-	-	-	B_4	10.2	6.8	66.5		10.4	4.9	47.6
A_5	8.6	5.3	61.6		13.8	8.7	62.9		14.9	4.9	33.2
A_6	-	-	-		20.9	10.9	52.1		16.5	10.9	65.9
A_7	8.2	2.9	35.1		21.1	11.2	53.0		16.4	9.9	60.5
A_8	-	-	-	B_5	15.3	4.9	32.2	C_3	19.2	17.2	89.6
	22.9	11.5	50.1		19.3	5.6	28.8		12.2	4.5	36.7
	25.4	12.8	50.1		20.9	7.1	34.1		8.2	4.6	56.5
A_9	23.4	19.9	85.1		19.4	6.2	31.8		8.6	6.4	74.6
	24.2	21.4	88.1		21.3	17.4	81.8				
	11.9	2.8	23.2		18.6	12.4	66.8				
	21.9	6.5	29.7	B_6	16.3	9.9	60.9				
A_10	25.6	15.1	58.8		19.0	13.1	68.8				
	10.6	4.9	46.7		16.3	11.2	68.6				
					19.5	13.1	67.0				

Table S4: The results of parameter calibration in experiments A, B and C with different numbers of pedestrians, respectively. The parameters sets listed in this table minimised *dist* (see main text) for each scenario, respectively.

Scenario	N	θ	δ	α	β
A	18	0.5	-1	0	4
A	40	0.9	-2	2	0
A	138	0.5	-2	0	10
B	11	0.7	0.5	10	10
B	40	0.05	2	2	8
B	138	0.15	-2	2	4
C	69	0.3	0.1	0	10
C	138	0.3	-2	0	0

3. JuPedSim – an open pedestrian simulation framework

All modelling and simulation tasks presented in this manuscript have been performed in the Jülich Pedestrian Simulator (JuPedSim). JuPedSim is a framework, mostly written in C++, for modelling and simulating pedestrian egress. It works in a 3-dimensional continuous environment. JuPedSim implements state of the art models and analysis methods. It is constructed around three loosely coupled software engines: a simulation engine, a visualisation engine and a reporting engine. We will briefly describe these three engines in the following.

The **simulation engine** simulates the movement of pedestrians given a geometry (e.g. room layout) and an initial configuration. The initial configuration includes the desired destinations, speeds, route choices and other demographic parameters about pedestrians such as the size and gender. The simulation modules implemented follow the strategic/tactical/operation levels paradigm for route choice at different spatio-temporal levels [S4] and allows the rapid prototyping of new models.

Three models at the tactical level (route choice, short term decisions) are already implemented in the framework: a shortest path strategy using the Dijkstra algorithm, a quickest path based on visibility and jam avoidance and a cognitive map, giving agents the possibility to explore the environment and discover doors for instance [S1]. In addition, some behavioural features are implemented, such as the possibility to share information about closed doors with other agents and the ability to explore an unknown environment when looking for an exit.

On the operational level (locomotion system, collision avoidance) JuPedSim implements three different force-based models: The ‘Generalized Centrifugal Force Model’ [S5], the ‘Gompertz model’ [S3] and a collision free first order model [S2]. The Gompertz model is based on a continuous physical force. Depending on the chosen parameter, the model simulates social, as well as physical forces, in a continuous way. This is in contrast to other known physical forces which are defined as a step-function to hinder excessive overlapping of pedestrians. All inputs follow a normal distribution.

The **reporting engine** analyses the trajectories from simulations or any other sources, such as empirical data. The module integrates four measurement methods. Possible analyses include pedestrian densities, velocities and flows in a given geometry.

The **visualisation engine** reads a file containing the simulation results (coordinates, velocities, orientations) together with geometry information and allows the user to interact with this information in form of an animation, for instance focusing on an area of interest or masking views. It can also be used in an online mode, where simulation results are directly streamed to the application.

JuPedSim emphasises the validation of the implemented models. The empirical data used for the validation come from numerous experiments that have been organized in different geometries. All inputs

and output files are XML based. JuPedSim is platform-independent and released under the LGPL License. In the following sections, we provide additional details about the modelling components presented in the main manuscript. For all additional parameters that are not reported in the main text, we use default values that can be found in reference [S3].

3.1 Visibility criteria

In many steps during the route choice process, the visibility between pedestrians and/or exits is computed. The inter-pedestrian visibility is determined by drawing a straight line joining the centre of both pedestrians and computing if this line intersects with other pedestrians or obstacles. Pedestrians are represented as circles with pre-defined radii. If desired, one could define pedestrians with different demographics parameters, relating to their size or desired velocity. All obstacles (e.g. walls) are represented by closed polygons. For visibility between a pedestrian and an exit, we consider the line between the centre of the exit and the centre of the pedestrian and check for occlusion with other pedestrians and/or obstacles. In this procedure, pedestrians queuing in front of the exit for which visibility is assessed are not considered (assuming that under these conditions, the queue in front of an exit is as informative as seeing the exit itself).

3.2 Selection of a reference pedestrian

When pedestrians are stuck in a jam or when they enter a new location (e.g. after passing through an exit), they select a reference pedestrian and estimate their new travel time. We define a pedestrian to be in a jam if his/her desired speed is not achieved. The selection of reference pedestrians is completed in two steps. First, the appropriate queues for the relevant exits are identified. The queues are made up of pedestrians who have the same destination, such as an exit door. For pedestrians to be eligible to be selected as reference pedestrians, they must be closer to this immediate destination than the pedestrian performing the estimation. In the second step, a reference pedestrian is selected from that queue by identifying the closest pedestrian in the visibility range of the pedestrian performing the estimation. The travel time is then estimated using equation 1 presented in the main manuscript.

3.3 Operational model

The operational model which controls the locomotion and collision avoidance of pedestrians in our simulations is a first order velocity based model:

$$\dot{X}_i = V \left(s_i(X_i, X_j, \dots) \times e_i(X_i, X_j, \dots) \right). \quad (\text{S2})$$

V is a piecewise linear function defining the optimal velocity which guarantees a collision-free minimal spacing in front of the pedestrian. s_i is the minimal space between a pedestrian and those in front of him/her. e_i defines the direction of the pedestrian (see equation S2), which is a combination of the desired direction e_0 given by the route choice model presented in the main manuscript and the relative vectors to other pedestrians in the walking direction. In this equation, N is a normalisation coefficient to ensure that e_i is a unit vector and R is a repulsive function which exponentially decays with increasing spacing with pedestrians in the front. This approach is a simplified version of the gradient navigation model [S6].

$$e_i(X_i, X_j, \dots)_i = \frac{1}{N} (e_0 + \sum_j R(S_{i,j}) e_{i,j}) \quad (\text{S3})$$

The two equations ensure a collision-free movement of pedestrians. More details on this models are presented in [S2].

4. Experimental data on pedestrian trajectories

Pedestrian trajectories for 10 runs in experiment A, 6 runs in experiment B and 3 runs in experiment C are provided in the supplementary files ‘trajectory_A.txt’, ‘trajectory_B.txt’ and ‘trajectory_C.txt’, respectively. Five columns are listed in each file.

- The first column is entitled ‘ID’, which represents the pedestrian ID in each run.
- The second column is entitled ‘Frame’, which records the current frame of each pedestrian. The frame rate for all experimental runs is 16 per second.
- The third and fourth columns are entitled ‘X [m]’ and ‘Y [m]’, which represent the pedestrian coordinates in metres. The coordinates of the origin (0,0) in experiments A, B and C are marked by the blue cross in figure 1 (d), (e) and (f) in the main text, respectively.
- The last column is entitled ‘Choice of exit’, which illustrates pedestrians’ target exits in each frame. In experiment A and C, ‘1’ represents the left exit and ‘2’ represents the right one; in experiment B, ‘1’, ‘2’, ‘3’ and ‘4’ represent the left, right, top and bottom exits, respectively (see figure 1d-f in the main text). ‘0’ represents that pedestrians have not made a decision.

References

- [S1] Haensel D. 2014 A knowledge-based routing framework for pedestrian dynamics simulation. *Master thesis, Technische Universität Dresden, November 2014.*
- [S2] Tordeux A, Chraibi M, Seyfried A. 2016 Collision-free speed model for pedestrian dynamics. In *Traffic and Granular Flow'15*, 28-30 October, Delft, Netherlands.
- [S3] Kemloh Wagoum AU, Chraibi M, Zhang J. 2015 JuPedSim: an open framework for simulating and analyzing the dynamics of pedestrians. In *3rd Conference of Transportation Research Group of India*, 17-20 December, Kolkata, India.
- [S4] Hoogendoorn SP, Bovy PHL, Daamen W. 2002 Microscopic pedestrian wayfinding and dynamics modelling. In *Pedestrian and Evacuation Dynamics 2002*, pp. 123-155.
- [S5] Chraibi M, Kemloh Wagoum AU, Seyfried A, Schadschneider A. 2011 Force-based models of pedestrian dynamics. *Networks and Heterogeneous Media* **6**, 425-442. (doi:10.3934/nhm.2011.6.425)
- [S6] Dietrich F, Köster G. 2014 Gradient navigation model for pedestrian dynamics. *Physical Review E* **89**, 062801. (doi:10.1103/PhysRevE.89.062801)